ELSEVIER

Mathematics and Computers in Simulation 55 (2001) 93–102

MATHEMATICS AND COMPUTERS IN SIMULATION

www.elsevier.nl/locate/matcom

The Monte Carlo method for semi-classical charge transport in semiconductor devices

H. Kosina*, M. Nedjalkov[1]

Institute for Microelectronics, TU-Vienna, Gusshausstraße 27-29, A1040 Vienna, Austria

Abstract

A brief review of the semi-classical Monte Carlo method for semiconductor device simulation is given, covering the standard Monte Carlo algorithms, variance reduction techniques, the self-consistent solution, and the physical semiconductor model including band structure and scattering mechanisms. The link between physically-based Monte Carlo methods and the numerical method of Monte Carlo integration is considered. The integral representations and the conjugate equations are presented for the transient and the steady-state Boltzmann equation. From these equations the standard algorithms as well as a variety of new algorithms can be derived in a formal way.

Keywords: Monte Carlo method; Boltzmann equation; Semiconductor devices

1. Introduction

Over the last three decades the Monte Carlo (MC) method has evolved to a reliable and frequently used tool which has been successfully employed to investigate a great variety of transport phenomena in semiconductors.

The method consists of a simulation of the motion of charge carriers in the six-dimensional phase space formed by the position and wave vectors. Subjected to the action of an external force, the point-like carriers follow trajectories determined by Newton's law and the carrier's dispersion relation. Due to imperfections of the crystal lattice the drift process is interrupted by scattering events, which are considered to be local in space and instantaneous in time. The duration of a drift process and the type of scattering mechanism are selected randomly according to given probabilities which describe the microscopic process.

In principle, such a procedure yields the carrier distribution in phase space. Integrating the distribution function over some phase space volume gives a measure for the relative number of carriers in that volume. Macroscopic quantities are obtained as mean values of the corresponding single-particle quantities. Moreover, the distribution function satisfies a Boltzmann equation (BE).

* Corresponding author.

[1] Permanent address: CLPP, BAS, G.Bontchev Str. B125A, 1113 Sofia, Bulgaria.

0378-4754/01/$20.00
PII: S0378-4754(00)00249-4

The method of generating sequences of drift and scattering appears so transparent from a physical point of view that it is frequently interpreted as a direct emulation of the physical process rather than as a numerical method. The main MC algorithms used to date were originally devised from merely physical considerations, viewing a MC simulation as a simulated experiment. The prove that the used algorithms implicitly solve the BE was carried out later.

The alternative way to use the BE explicitly and to formulate MC algorithms for its solution was reported only one decade ago in the literature. New MC algorithms are derived which typically differ from the common ones by the fact that additional statistical variables appear, such as weights, that do not have a counterpart in the real statistical process.

2. Application of the MC method to semiconductor devices

Based upon the physical picture of the MC technique it has been possible to apply the method to the simulation of a great variety of semiconductor devices. When the need for variance reduction techniques emerged these have again been devised from physical considerations, like splitting a particle into light ones by conserving the charge. For the MC simulation of devices there are two algorithms generally employed, known as the ensemble MC (EMC) and the one particle MC (OPMC) algorithms.

2.1. MC algorithms

For a systematic description of the MC algorithms let us begin with the homogeneous case. Transient phenomena are due to the evolution of the carrier system from an initial to some final distribution. Accordingly, the evolution of an ensemble of test particles is simulated starting from a given initial condition. The physical characteristics are obtained in terms of ensemble averages, giving rise to the name Ensemble MC [1,2]. For example, the distribution function in a given phase space point at a given time is estimated as the relative number of particles in a small volume around the point.

The EMC algorithm can also be applied under stationary conditions. In this situation, for large evolution times the final distribution approaches a steady-state, and the information introduced by the initial condition is lost entirely. Alternatively, the ergodicity of the process can be exploited to replace the ensemble average by a time average. Since it is sufficient to simulate one test particle for a long period of time, the algorithm is called one-particle MC. The distribution function in a given phase space point is estimated by the time spent by the particle in a fixed, small volume around the point divided by the total time the trajectory was followed. The effect of the particle's initial state vanishes for long simulation times. Another method of obtaining steady-state averages has been introduced by Price [3]. With the *synchronous-ensemble* or *before-scattering* method averages are formed by sampling the trajectory at the end of each free flight, which is in many cases easier a task than evaluating a path integral over each free flight. When the EMC algorithm is applied to the simulation of a stationary phenomenon, the steady-state is reached after the initial transient has decayed. The ensemble average is taken at the end of the simulation time, while, on the contrary, with the OPMC algorithm averages are recorded during the whole time of simulation.

For the inhomogeneous situation the mathematical model needs to be augmented by boundary conditions. A Neumann type of boundary is simply realized by reflecting the particles at the boundary. Physical models for Ohmic contacts typically enforce local charge neutrality [4]. The EMC and the OPMC

algorithms remain basically unchanged in the inhomogeneous case. Whenever in an OPMC simulation a particle leaves the simulation domain through an Ohmic contact it is re-injected through one of the contacts, selected according to the probabilities of the underlying model.

It has been proven that the described algorithms yield a distribution function which satisfy the respective BE. Fawcett et al. have shown that the homogeneous OPMC leads to the steady-state BE [5], whereas Baccarani et al. gave this proof for the inhomogeneous OPMC [6]. A proof originally given by Reklaitis [7] and also reported in [8] demonstrates that the homogeneous EMC renders the transient BE.

The established technique to study the small signal AC characteristics of a device consists of an EMC simulation of the transient response. Elements of the impedance matrix are obtained by applying a steplike voltage signal at a given port, and calculating the Fourier transform of the response currents through all ports of interest. Since the EMC simulation captures the general nonlinear behavior of a device the voltage increment must be sufficiently small in order to stay in the linear response regime. A MC algorithm for the solution of the BE linearized with respect to the field would have significant advantages over the above described method. Yet to date such algorithms exist only for the homogeneous case. MC algorithms for small signal analysis are reported in [9–12]. Reviews can be found in [13,14].

2.2. Physical models

The work of Kurosawa in 1966 [15] is considered as the first account of an application of the MC method to high-field transport in semiconductors. The following decade has seen considerable improvement of the method and application to a variety of materials [4]. Early papers deal with gallium arsenide [5] and germanium [16]. In the mid 1970s a physical model of silicon has been developed, capable of explaining major macroscopic transport characteristics [17,18]. The used band structure models were represented by simple analytic expressions accounting for non-parabolicity and anisotropicity. With the increase of the energy range of interest then the need for accurate, numerical band structure models arose [19–22]. For electrons in silicon, the most thoroughly investigated case, it is believed that only recently a satisfactory understanding of the basic scattering mechanisms at high energies has been reached, giving rise to a new ‘standard model’ [23]. Various technologically significant semiconductors and alloys are investigated in [24].

Several attempts were made to circumvent the usage of the full, anisotropic band structure by employing simpler, analytic band models whose free parameters are fixed by best fitting a given density of states [25–27]. Although having such models of intermediate complexity is very desirable, a comparative study, however, revealed that they fall to reproduce the high energy part of the distribution function [28].

The interaction of the carriers with the crystal imperfections is generally considered as weak enough such as to allow a treatment by the so-called *golden rule* of quantum mechanics, an outcome of first order, time-dependent perturbation theory. Dominant scattering mechanisms are due to various modes of thermal lattice vibrations, ionized impurities [29,30], and at high energies impact ionization [19,31–33]. Other mechanisms, such as plasmon scattering [34,35] and carrier–carrier scattering [36], as well as the Pauli exclusion principle [37,38] make the transport problem strongly nonlinear.

2.3. Self-consistent coupling schemes

In a semiconductor device the particles move in an electric field that originates from fixed background charges and from the charge carried by the particles themselves. In a simulation a self-consistent solution of the transport problem and the Poisson equation is achieved by means of iteration. On each step the

particle-mesh force calculation is carried out, consisting of four principal steps: (1) assign the charge to the mesh, (2) solve the field equation on the mesh, (3) calculate the mesh-defined force field, and, (4) interpolate to find forces on the particles [1]. Compared with OPMC, stability requirements for EMC are more severe. Problems associated with self-consistent EMC simulation are the avoidance of self-forces [1,39] and the proper choice of the field-adjusting time step. The latter needs to be in accordance with the Nyquist theorem, where the highest frequency to be sampled is given by the plasmon frequency [20]. The high frequency of required field updates calls for fast Poisson solvers [1]. EMC is coupled with the linear Poisson equation via the particle density.

In case of OPMC a stable, self-consistent iteration scheme is obtained by using the quasi-Fermi level and the carrier temperature from the MC simulation in the Poisson equation, which is nonlinear in this case due to the chosen variable set [40]. The so-called *MC-drift-diffusion* coupling technique provides another scheme for self-consistent iteration [41]. From the particle simulation transport coefficients are extracted, which are then used in a drift-diffusion like current relation. In each iteration step the coupled set of semiconductor equations is solved, consisting of the Poisson and the carrier continuity equations [42].

In surface inversion layers or channels formed by hetero junctions the motion of the carriers normal to the interface is quantized and thus governed by the Schrödinger equation [43]. The coupled solution of MC transport parallel to the interface, Poisson equation, and Schrödinger equation needs to be sought. Self-consistency has to be achieved for the potential, the eigen-energies, and sub-band populations. The strengths of the scattering mechanisms are modified through the overlap integrals [44–47].

2.4. Variance reduction techniques

The large variations of the carrier density within a realistic device impose severe problems upon the common MC algorithms. Statistical enhancement methods are required to reduce the variance in rarely visited phase space regions of interest. Trajectory multiplication schemes used in various MC device simulators [42,48,49] are extensions of the method of Phillips and Price [50]. Several variable-weight or population control techniques have been developed for the EMC [51–54]. A comparison of statistical enhancement methods is given in [55].

3. MC algorithms for the solution of the Boltzmann equation

The alternative way, namely to state the transport equation first and to formulate then a MC algorithm for its solution, was reported only one decade ago [56,57]. A link between physically-based MC methods and numerical MC methods for solving integrals and series of integrals could be established.

In [56] the BE is transformed into an integral equation which is then iteratively substituted into itself. The resulting iteration series is evaluated by a new MC technique, called MC Backward (MCB) since the trajectories are followed back in time. All trajectories start from the chosen phase space point, and their number is freely adjustable and not controlled by the physical process. MCB allows for the evaluation of the distribution function in a given point with a desired precision. The algorithm can be useful when simulating rare events or when the distribution function is needed only in a small phase space domain.

The weighted ensemble MC (WEMC) method allows the use of arbitrary probabilities for trajectory construction, such that particles can be guided toward to a region of interest [58,59]. The method evaluates the iteration series of an integral form of the BE originally given by Chambers [60]. The unbiased estimator

for the distribution function contains a product of weights which are given by the ratio of the real and the modified probabilities of the selected events.

With the iteration approach presented in [57] the MCB and the WEMC algorithms are stated in an unified way. The concept of numerical trajectories is introduced. The common EMC algorithm is obtained as a particular case, in which the numerical trajectories coincide with the physical carrier trajectories, for homogeneous [61] and inhomogeneous [62] conditions.

3.1. Introduction to integral equations

The semi-classical transport problem in semiconductors can be formulated in terms of a Fredholm integral equation of the second kind for the distribution function f:

$$f(x) = \int f(x')K(x', x)\,\mathrm{d}x' + f_0(x) \tag{1}$$

The kernel K and the free term f_0 are given functions. The multi-dimensional variable x will denote $(\boldsymbol{k}, \boldsymbol{r}, t)$ in the transient case and $(\boldsymbol{k}, \boldsymbol{r})$ in the steady state. The iteration

$$f^{(0)}(x) = f_0(x) \tag{2}$$

$$f^{(n+1)}(x) = \int f^{(n)}(x')K(x', x)\,\mathrm{d}x' \tag{3}$$

gives a formal solution to Eq. (1), known as the *Neumann series*:

$$f = f^{(0)} + f^{(1)} + f^{(2)} + \cdots \tag{4}$$

For our purposes it will be convenient to consider also the integral equation conjugate to Eq. (1)

$$g(x') = \int g(x)K(x', x)\,\mathrm{d}x + g_0(x) \tag{5}$$

It can be easily shown, that the following relation holds, where a scalar product $(u, v) = \int u(x)v(x)\,\mathrm{d}x$ is used:

$$(f, g_0) = (g, f_0) \tag{6}$$

The link with the MC method is established by approaching the terms of the Neumann series by MC integration. Consider the task of evaluation of an integral

$$I = \int_{-\infty}^{\infty} \phi(x)\,\mathrm{d}x = \int_{-\infty}^{\infty} p(x)\psi(x)\,\mathrm{d}x \tag{7}$$

where ϕ is absolutely integrable. Suppose that $\phi = p\psi$, where p is nonnegative and $\int_{-\infty}^{\infty} p(x)\,\mathrm{d}x = 1$, which means that p is a density function. Then I is the expectation value of ψ with respect to the density p: $I = E_p\{\psi\}$. A MC estimate for I is obtained by generating a sample $\{x_1, \ldots, x_N\}$ from the density p, and taking the sample mean $\bar{\psi} = N^{-1}\sum_{i=1}^{N}\psi(x_i)$. After the central limit theorem the sample mean approaches I for $N \to \infty$.

In the following sections the linear BE is considered. The integral forms and the conjugate equations are given both for the transient and the steady-state problem. Examples for the iteration terms of the Neumann series are shown.

3.2. The initial value problem

In the inhomogeneous, transient case the distribution function depends on the seven-dimensional variable $(\boldsymbol{k}, \boldsymbol{r}, t)$. The commonly used integral form of the BE (see, e.g. [62]) transforms after a straight-forward augmentation into the standard form (1):

$$f(\boldsymbol{k}, \boldsymbol{r}, t) = \int_0^\infty \mathrm{d}t' \int \mathrm{d}\boldsymbol{k}' \int \mathrm{d}\boldsymbol{r}' f(\boldsymbol{k}', \boldsymbol{r}', t') K(\boldsymbol{k}', \boldsymbol{r}', t', \boldsymbol{k}, \boldsymbol{r}, t) + f_0(\boldsymbol{k}, \boldsymbol{r}, t) \tag{8}$$

The kernel and the free term are defined as follows:

$$K(\boldsymbol{k}', \boldsymbol{r}', t', \boldsymbol{k}, \boldsymbol{r}, t) = S(\boldsymbol{k}', \boldsymbol{K}(t'), \boldsymbol{r}', t') \exp\left(-\int_{t'}^{t} \lambda(\boldsymbol{K}(y), \boldsymbol{R}(y), y)\,\mathrm{d}y\right) \delta(\boldsymbol{r}' - \boldsymbol{R}(t'))\theta(t - t') \tag{9}$$

$$f_0(\boldsymbol{k}, \boldsymbol{r}, t) = f_\mathrm{i}(\boldsymbol{K}(0), \boldsymbol{R}(0)) \exp\left(-\int_0^t \lambda(\boldsymbol{K}(y), \boldsymbol{R}(y), y)\,\mathrm{d}y\right) \tag{10}$$

where S denotes the differential scattering rate and f_i the initial distribution function.

The trajectory $(\boldsymbol{K}, \boldsymbol{R})$ is a solution of the equations of motion with the initial condition $\boldsymbol{K}(t) = \boldsymbol{k}$, $\boldsymbol{R}(t) = \boldsymbol{r}$:

$$\boldsymbol{K}(\tau) = \boldsymbol{k} + \int_t^\tau \boldsymbol{F}(\boldsymbol{R}(y))\,\mathrm{d}y, \qquad \boldsymbol{R}(\tau) = \boldsymbol{r} + \int_t^\tau \boldsymbol{v}(\boldsymbol{K}(y))\,\mathrm{d}y \tag{11}$$

The force field $\hbar\boldsymbol{F}$ can be due to electric and magnetic fields. The carrier's group velocity $\boldsymbol{v}$ is related to the band energy $\epsilon(\boldsymbol{K})$ by $\boldsymbol{v} = \hbar^{-1}\nabla_k \epsilon(\boldsymbol{k})$.

The common integro-differential form of the BE is recovered from Eq. (8) by performing the $\boldsymbol{r}'$ integration, replacing the upper bound of the time integral by t thus eliminating the unit step function, and taking the total time derivative.

As an example, we explicitly write the term $f^{(2)}$ of the Neumann series (4)

$$\begin{aligned} f^{(2)}(\boldsymbol{k}, \boldsymbol{r}, t) = \int_0^t \mathrm{d}t_1 \int \mathrm{d}\boldsymbol{k}_1 \int_0^{t_1} \mathrm{d}t_2 \int \mathrm{d}\boldsymbol{k}_2\, f_\mathrm{i}(\boldsymbol{K}_2(0), \boldsymbol{R}_2(0)) \exp\left(-\int_0^{t_2} \lambda(\boldsymbol{K}_2(y), \boldsymbol{R}_2(y), y)\,\mathrm{d}y\right) \\ \times S(\boldsymbol{k}_2, \boldsymbol{K}_1(t_2), \boldsymbol{R}_1(t_2), t_2) \exp\left(-\int_{t_2}^{t_1} \lambda(\boldsymbol{K}_1(y), \boldsymbol{R}_1(y), y)\,\mathrm{d}y\right) \\ \times S(\boldsymbol{k}_2, \boldsymbol{K}(t_1), \boldsymbol{R}(t_1), t_1) \exp\left(-\int_{t_1}^{t} \lambda(\boldsymbol{K}(y), \boldsymbol{R}(y), y)\,\mathrm{d}y\right) \end{aligned} \tag{12}$$

The real space trajectory is continuous at the time of scattering, e.g. $\boldsymbol{R}_2(t_2) = \boldsymbol{R}_1(t_2)$, and the initial conditions for the $\boldsymbol{k}$-space trajectories are given by the before-scattering states, e.g. $\boldsymbol{K}(t_2) = \boldsymbol{k}_2$. Evaluation of iteration terms of the form (12) by MC integration leads to the MCB algorithm. Since $\boldsymbol{k}, \boldsymbol{r}, t$ are given, the construction of the numerical trajectory starts at this point by choosing a random variable t_1, which obviously is less than t. The next random variable to be chosen is $\boldsymbol{k}_1$, a before-scattering state, and so forth. This means that the numerical trajectory is followed back in time.

With the kernel (9) the conjugate Eq. (5) becomes

$$g(\boldsymbol{k}', \boldsymbol{r}', t') = \int_{t'}^{\infty} \mathrm{d}\tau \int \mathrm{d}\boldsymbol{k}_a \, S(\boldsymbol{k}', \boldsymbol{k}_a, \boldsymbol{r}', t') \exp\left(-\int_{t'}^{\tau} \lambda(\boldsymbol{K}(y), \boldsymbol{R}(y), y)\, \mathrm{d}y\right) g(\boldsymbol{K}(\tau), \boldsymbol{R}(\tau), \tau) + g_0(\boldsymbol{k}', \boldsymbol{r}', t') \tag{13}$$

To obtain this result, in the kernel (9) variables are changed: $\boldsymbol{k}_a = \boldsymbol{K}(t')$, $\boldsymbol{r}'' = \boldsymbol{R}(t')$. According to the Liouville theorem the volume element does not change over a trajectory: $\mathrm{d}\boldsymbol{k}\,\mathrm{d}\boldsymbol{r} = \mathrm{d}\boldsymbol{k}_a\,\mathrm{d}\boldsymbol{r}''$. The $\boldsymbol{r}''$ integration is then carried out with the help of the δ-function.

For a particular choice of the free term, $g_0 = \delta(\boldsymbol{k}-\boldsymbol{k}')\delta(\boldsymbol{r}-\boldsymbol{r}')\delta(t-t')$, g represents the Green function. Using Eq. (6) the solution of Eq. (8) is obtained by the scalar product

$$f(\boldsymbol{k}, \boldsymbol{r}, t) = \int_0^{\infty} \mathrm{d}t' \int \mathrm{d}\boldsymbol{k}' \int \mathrm{d}\boldsymbol{r}' \, g(\boldsymbol{k}', \boldsymbol{r}', t')\, f_0(\boldsymbol{k}', \boldsymbol{r}', t') \tag{14}$$

Assume that we are interested in the integral of f over some subdomain Ω at time t: $f_\Omega(t) = \int_0^{\infty}\mathrm{d}t' \int \mathrm{d}\boldsymbol{k}' \int \mathrm{d}\boldsymbol{r}'\, f(\boldsymbol{k}', \boldsymbol{r}', t')\delta(t-t')\theta_\Omega(\boldsymbol{k}', \boldsymbol{r}')$, where θ_Ω denotes the indicator function of the subdomain. From $f_\Omega(t) = (f, g_0)$ the free term is obtained as $g_0 = \delta(t-t')\theta_\Omega(\boldsymbol{k}', \boldsymbol{r}')$. Using the Neumann series of Eq. (13), $g = \sum_0^{\infty} g(i)$, we obtain $f_\Omega(t) = (f_0, g) = \sum_0^{\infty} f_\Omega^{(n)}$. After some algebra the second order term can be written as

$$\begin{aligned} f_\Omega^{(2)} = {} & \int_0^t \mathrm{d}t_2 \int_{t_2}^t \mathrm{d}t_1 \int_t^{\infty} \mathrm{d}t_0 \int \mathrm{d}\boldsymbol{k}_2^a \int \mathrm{d}\boldsymbol{k}_1^a \int \mathrm{d}\boldsymbol{k}_i \int \mathrm{d}\boldsymbol{r}_i \{f_\mathrm{i}(\boldsymbol{k}_i, \boldsymbol{r}_i)\} \\ & \times \left\{\lambda(\boldsymbol{K}_2(t_2), \boldsymbol{R}_2(t_2), t_2) \exp\left(-\int_0^{t_2} \lambda(\boldsymbol{K}_2(y), \boldsymbol{R}_2(y), y)\mathrm{d}y\right)\right\} \left\{\frac{S(\boldsymbol{K}_2(t_2), \boldsymbol{k}_2^a, \boldsymbol{R}_2(t_2), t_2)}{\lambda(\boldsymbol{K}_2(t_2), \boldsymbol{R}_2(t_2), t_2)}\right\} \\ & \times \left\{\lambda(\boldsymbol{K}_1(t_1), \boldsymbol{R}_1(t_1), t_1) \exp\left(-\int_{t_2}^{t_1} \lambda(\boldsymbol{K}_1(y), \boldsymbol{R}_1(y), y)\mathrm{d}y\right)\right\} \left\{\frac{S(\boldsymbol{K}_1(t_1), \boldsymbol{k}_1^a, \boldsymbol{R}_1(t_1), t_1)}{\lambda(\boldsymbol{K}_1(t_1), \boldsymbol{R}_1(t_1), t_1)}\right\} \\ & \times \left\{\lambda(\boldsymbol{K}(t_0), \boldsymbol{R}(t_0), t_0) \exp\left(-\int_{t_1}^{t_0} \lambda(\boldsymbol{K}(y), \boldsymbol{R}(y), y)\mathrm{d}y\right)\right\} \theta_\Omega(\boldsymbol{K}(t), \boldsymbol{R}(t)) \end{aligned} \tag{15}$$

This term describes the path of a particle that undergoes two scattering events within the given time interval (0, t) and hence passes time t on its third free flight. In Eq. (15) the expressions enclosed in curly brackets match exactly those probability densities used in the EMC algorithm. Note that $\lambda^{-1}S$ is the normalized distribution of the after-scattering states: $\int \lambda^{-1}(\boldsymbol{k})S(\boldsymbol{k}, \boldsymbol{k}')\,\mathrm{d}\boldsymbol{k}' = 1$. To evaluate Eq. (15) by MC integration one have to generate N realizations of the multi-dimensional variable $\{\boldsymbol{k}_i, \boldsymbol{r}_i, t_2, \boldsymbol{k}_2^a, t_1, \boldsymbol{k}_1^a, t_0\}$ which is termed a numerical trajectory. One would first generate a phase space point $(\boldsymbol{k}_i, r_i)$ from the initial distribution f_i, then choose t_2 from the free flight time distribution, select $\boldsymbol{k}_2^a$ with density $\lambda^{-1}S$, and so forth. Finally, at time t the indicator function θ_Ω, which plays the role of ψ in Eq. (7), needs to be evaluated. The result will be simply 1 or 0. Doing so for N trajectories corresponds to counting the number of particles found in Ω at time t.

The generated times are of ascending order, $0 < t_2 < t_i < t_0$, and the generated wave vectors are after scattering states, which means that the trajectory is followed forward in time. With a forward algorithm it is possible only to evaluate the average of the distribution function over some subdomain rather than the exact value in a given point. Only the MCB algorithm is capable of evaluating the distribution function point-wise.

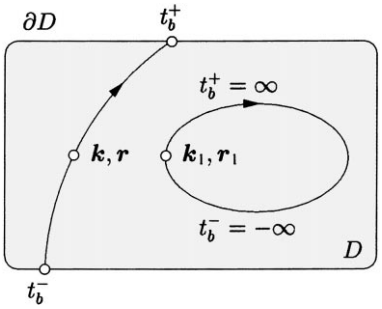

Fig. 1. Illustration of the functions $t_\mathrm{b}^-(\boldsymbol{k},\boldsymbol{r})$ and $t_\mathrm{b}^+(\boldsymbol{k},\boldsymbol{r})$, which give the time at the trajectory's entry point and exit point, respectively. If $(\boldsymbol{k}_1,\boldsymbol{r}_1)$ is the initial point of a closed trajectory, the times are $t_\mathrm{b}^\pm(\boldsymbol{k}_1,\boldsymbol{r}_1) = \pm\infty$.

In the Weighted EMC technique instead of the physical densities in Eq. (15), which follow in a natural way from the kernel, arbitrary densities are used for numerical trajectory construction. The ratio of the physical density over the numerical density appears in the integrand.

3.3. The boundary-value problem

In the inhomogeneous, steady-state case the integral equation is defined in the six-dimensional phase space. The position vector is restricted to the simulation domain D:

$$f(\boldsymbol{k},\boldsymbol{r}) = \int \mathrm{d}\boldsymbol{k}' \int \mathrm{d}\boldsymbol{r}'\, f(\boldsymbol{k}',\boldsymbol{r}') K(\boldsymbol{k}',\boldsymbol{r}',\boldsymbol{k},\boldsymbol{r}) + f_0(\boldsymbol{k},\boldsymbol{r}) \tag{16}$$

The kernel and the free term are defined as follows, where f_b denotes the distribution function at the boundary:

$$K(\boldsymbol{k}',\boldsymbol{r}',\boldsymbol{k},\boldsymbol{r}) = \int_{t_\mathrm{b}^-(\boldsymbol{k},\boldsymbol{r})}^{0} \mathrm{d}t' S(\boldsymbol{k}', \boldsymbol{K}(t'), \boldsymbol{r}') \exp\left(-\int_{t'}^{0} \lambda(\boldsymbol{K}(y), \boldsymbol{R}(y))\,\mathrm{d}y\right) \delta(\boldsymbol{r}' - \boldsymbol{R}(t')) \tag{17}$$

$$f_0(\boldsymbol{k},\boldsymbol{r}) = f_\mathrm{b}(\boldsymbol{K}(t_\mathrm{b}^-), \boldsymbol{R}(t_\mathrm{b}^-)) \exp\left(-\int_{t_\mathrm{b}^-(\boldsymbol{k},\boldsymbol{r})}^{0} \lambda(\boldsymbol{K}(y), \boldsymbol{R}(y))\,\mathrm{d}y\right) \tag{18}$$

The trajectory $(\boldsymbol{K}, \boldsymbol{R})$ is a solution of the equations of motion with the initial condition $\boldsymbol{K}(0) = k$, $\boldsymbol{R}(0) = \boldsymbol{r}$. The functions $t_\mathrm{b}^-(\boldsymbol{k},\boldsymbol{r})$ and $t_\mathrm{b}^+(\boldsymbol{k},\boldsymbol{r})$ denote the times when the trajectory enters and leaves, respectively, the simulation domain (see Fig. 1).

From the Neumann series of Eq. (16) it is possible to derive a steady-state, backward MC algorithm. First results show, that both the before-scattering and the time-recording method for average recording, known from the (forward) OPMC, are also available. Details of the new algorithm will be published in forthcoming paper.

The formal derivation of the forward, steady-state algorithm (OPMC) starts from the conjugate equation:

$$g(\boldsymbol{k}',\boldsymbol{r}') = \int \mathrm{d}\boldsymbol{k}_a \int_0^{t_\mathrm{b}^+(\boldsymbol{k}_a,\boldsymbol{r}')} \mathrm{d}\tau\; S(\boldsymbol{k}', \boldsymbol{K}_1, \boldsymbol{r}') \exp\left(-\int_0^{\tau} \lambda(\boldsymbol{K}(y), \boldsymbol{R}(y))\mathrm{d}y\right) g(\boldsymbol{K}(\tau), \boldsymbol{R}(\tau)) + g_0(\boldsymbol{k}',\boldsymbol{r}')$$

It is possible to express the iteration terms in such a form that the probability densities used in the OPMC appear. The before-scattering and the time recording methods for average recording are obtained in a very natural way. The initial points of the trajectories have to generated with a velocity-weighted boundary distribution, $v_\perp f_\mathrm{b}$, where f_b is given and $v_\perp$ is the component of the velocity normal to the boundary.

4. Conclusion

As of to date the two standard Monte Carlo algorithms, which are widely used for Monte Carlo device simulation on a semi-classical level, are the ensemble and the one-particle algorithms. The insight in the physics of the transport process has improved tremendously. From the Boltzmann equation represented as an integral equation, generalized Monte Carlo algorithms can be derived, as has been demonstrated by the weighted ensemble and the backward algorithms. Although these algorithms have the potential to solve problems occurring in device simulation, such as coping with rare events, moving carriers over retarding energy barriers, or avoiding the simulation of too many trajectories in equilibrium regions where the distribution function is known, they have not been applied to realistic structures yet. The great freedom in choosing density functions for numerical trajectory construction opens a wide field for the development of new algorithms.

Acknowledgements

This work has been supported by the ‘Fonds zur Förderung der wissenschaftlichen Forschung’, project P 13333-TEC.

References

[1] R. Hockney, J. Eastwood, Computer Simulation Using Particles, Adam Hilger, Bristol, Philadelphia, 1988.
[2] C. Moglestue, Computer Methods Appl. Mech. Eng. 30 (1982) 173.
[3] P. Price, IBM J. Res. Develop. 14 (1970) 12.
[4] C. Jacoboni, P. Lugli, The Monte Carlo Method for Semiconductor Device Simulation, Springer, New York, 1989.
[5] W. Fawcett, A. Bodman, S. Swain, J. Phys. Chem. Solids 31 (1970) 1963.
[6] G. Baccarani, C. Jacoboni, A.M. Mazzone, Solid-State Electron. 20 (1977) 5.
[7] A. Reklaitis, Phys. Lett. 7 (1982) 367.
[8] L. Reggiani (Ed.), Hot-electron transport in semiconductors, Topics in Applied Physics, Vol. 58, Springer, Berlin, 1985.
[9] P. Lebwohl, J. Appl. Phys. 44 (1973) 1744.
[10] J. Zimmermann, Y. Leroy, E. Constant, J. Appl. Phys. 49 (1978) 3378.
[11] P. Price, J. Appl. Phys. 54 (1983) 3616.
[12] E. Starikov, P. Shiktorov, Sov. Phys. Semicond. 22 (1988) 45.
[13] J. Vaissiere, et al., Phys. Rev. B 49 (1994) 11144.
[14] T. Wang, K. Hess, G. Iafrate, J. Appl. Phys. 58 (1985) 857.
[15] T. Kurosawa, in: Proceedings of the 8th International Conference on Phys. Sem., Kyoto, Japan, J. Phys. Soc. Jpn. (1966) 424.
[16] W. Fawcett, E. Paige, J. Phys. C: Solid State Phys. 4 (1971) 1801.
[17] C. Canali, et al., Phys. Rev. B 12 (1975) 2265.
[18] C. Jacoboni, R. Minder, G. Majni, J. Phys. Chem. Solids 36 (1975) 1129.
[19] H. Shichijo, K. Hess, Phys. Rev. B 23 (1981) 4197.

[20] M. Fischetti, S. Laux, Phys. Rev. B 38 (1988) 9721.
[21] T. Knnikiyo, et al., J. Appl. Phys. 75 (1994) 297.
[22] P. Yoder, J. Higman, J. Bude, K. Hess, Semicond. Sci. Technol. 7 (1992) 357.
[23] M. Fischetti, S. Laux, in: G. Baccarani, M. Rudan (Eds.), Proceedings of the 26th European Solid State Device Research Conference, Editions Frontiers, Bologna, Italy, 1996, pp. 813–820.
[24] M. Fischetti, IEEE Trans. Electron Dev. 38 (1991) 634.
[25] R. Brunetti, et al., Solid-State Electron. 32 (1989) 1663.
[26] T. Vogelsang, W. Hänsch, J. Appl. Phys. 70 (1991) 1493.
[27] A. Abramo, et al., IEEE Trans. Computer-Aided Design 12 (1993) 1327.
[28] A. Abramo, et al., IEEE Trans. Electron Dev. 41 (1994) 1646.
[29] D. Chattopadhyay, H. Queisser, Rev. Modern Phys. 53 (1981) 745.
[30] H. Kosina, G. Kaiblinger-Grujin, Solid-State Electron. 42 (1998) 331.
[31] J. Tang, K. Hess, J. Appl. Phys. 54 (1983) 5139.
[32] N. Sano, T. Aoki, M. Tomizawa, A. Yoshii, Phys. Rev. B 41 (1990) 12–122.
[33] W. Grant, Solid-State Electron. 16 (1973) 1189.
[34] M. Fischetti, Phys. Rev. B 44 (1991) 5527.
[35] N. Mansour, K. Diff, K. Brennan, J. Appl. Phys. 80 (1996) 5770.
[36] N. Takenaka, M. Inone, Y. Inuishi, J. Phys. Soc. Jpn. 47 (1979) 4931.
[37] S. Bosi, C. Jacoboni, J. Phys. C C9 (1976) 315.
[38] P. Lugli, D. Ferry, IEEE Trans. Electron Dev. ED-32 (1985) 2431.
[39] S. Laux, IEEE Trans. Computer-Aided Design 15 (1996) 1266.
[40] F. Venturi, et al., in: G. Baccarani, M. Rudan (Eds.), Proceedings of the Symposium on Simulation of Semiconductor Devices and Processes, Tecnoprint, Bologna, 1988, pp. 383–386.
[41] S. Bandyopadhyay, et al., IEEE Trans. Electron Dev. ED-34 (1987) 392.
[42] H. Kosina, S. Selberherr, IEEE Trans. Computer-Aided Design 13 (1994) 201.
[43] T. Ando, A. Fowler, F. Stern, Rev. Mod. Phys. 54 (1982) 437.
[44] K. Yokoyama, K. Hess, Phys. Rev. B 33 (1986) 5595.
[45] M. Shirahata, K. Taniguchi, C. Hamaguchi, J. Appl. Phys. 9 (1987) 1447.
[46] C. Jungemann, A. Emunds, W. Engi, Solid-State Electron. 36 (1993) 1529.
[47] M. Fischetti, S. Laux, Phys. Rev. B 48 (1993) 2244.
[48] E. Sangiorgi, B. Ricco, F. Venturi, IEEE Trans. Computer-Aided Design 7 (1988) 259.
[49] F. Venturi, et al., IEEE Trans. Computer-Aided Design 8 (1989) 360.
[50] A. Phillips, P. Price, Appl. Phys. Lett. 30 (1977) 528.
[51] T. Wang, K. Hess, G. Iafrate, J. Appl. Phys. 58 (1985) 857.
[52] S. Laux, M. Fischetti, Numerical aspects and implementation of the DAMOCLES Monte Carlo device simulation program, in: K. Hess (Ed.), Monte Carlo Device Simulation: Full Band and Beyond, Kluwer Academic Publishers, Boston, 1991, pp. 1–26.
[53] M. Martin, T. González, D. Pardo, J. Velázquez, Semicond. Sci. Technol. 11 (1996) 380.
[54] C. Jungemann, et al., in: Proceedings of the Symposium on Simulation of Semiconductor Processes and Devices, Business Center for Academic Societies Japan, Tokyo, Japan, 1996, pp. 65–66.
[55] C. Wordelman, T. Kwan, C. Snell, IEEE Trans. Computer-Aided Design 17 (1998) 1230.
[56] C. Jacoboni, P. Poli, L. Rota, Solid-State Electron. 31 (1988) 5523.
[57] M. Nedjalkov, P. Vitanov, Solid-State Electron. 32 (1989) 893.
[58] C. Jacoboni, in: Proceedings of the International Electron Devices Meeting, IEEE Electron Devices Society, Washington, DC, 1989, pp. 469–472.
[59] L. Rota, C. Jacoboni, P. Poli, Solid-State Electron. 32 (1989) 1417.
[60] R. Chambers, Proc. Phys. Soc. London A 65 (1952) 458.
[61] M. Nedjalkov, P. Vitanov, Solid-State Electron. 33 (1990) 407.
[62] P. Vitanov, M. Nedjalkov, COMPEL 10 (1991) 531.